JOURNAL OF THERMOPHYSICS AND HEAT TRANSFER
Vol. 34, No. 2, April–June 2020

Temperature Synchronization of Natural Convection in Adjacent Thermostatically Controlled Cavities

M. Sanchez-Lopez,* R. Chavez-Martinez,† and F.J. Solorio‡
National Autonomous University of Mexico, 04510 Mexico City, Mexico
and
M. Sen§
University of Notre Dame, Notre Dame, Indiana 46556

https://doi.org/10.2514/1.T5663

This is an experimental study of the synchronization of temperatures in two adjacent cavities that share a common wall, with air as the working fluid. The temperature of each cavity is independently controlled using an on/off thermostat with a finite deadband. Each cavity also has a heater that turns on or off, leading to oscillations in the temperature. The temperature is measured in each cavity. Conduction through the common wall leads to thermal interaction between the cavities. Phase synchronization of the temperature oscillations is observed and, depending on system parameters, there is a phase shift between the oscillations.

Nomenclature

f_i	=	instantaneous frequency of temperature oscillation, Hz
R_e	=	electrical resistance, Ω
r	=	Kuramoto order parameter
T_c	=	temperature of environmental chamber, °C
T_L	=	lower limit of temperature in cavity, °C
T_U	=	upper limit of temperature in cavity, °C
$T_1(t)$	=	temperature of left cavity, °C
$T_2(t)$	=	temperature of right cavity, °C
TC_α	=	temperature control signal; position α, °C
TC_β	=	temperature control signal; position β, °C
ΔT	=	temperature difference between T_L and T_c, °C
ΔT_{db}	=	deadband, °C
$\Delta\phi$	=	phase difference between temperature oscillations, deg
τ	=	instant period, s
ϕ_i	=	instantaneous phase of temperature in cavity 1 or cavity 2, deg

I. Introduction

AROUND 40% of the energy produced in developed countries is used for the thermal conditioning of houses and buildings [1,2], and this proportion is increasing. For this reason, diminishing energy usage is of relevance not only to decrease operational costs but also to reduce our environmental footprint. Diverse studies have been carried out to improve the efficiency of Heating, Ventilation, and Air Conditioning (HVAC) systems [3], to create new building materials, and to improve the thermal insulation in buildings [4–6]. Here, experiments have been carried out to study the effect of thermal interaction in spaces separated by common walls, as well as its effect on energy consumption. It is thought that in-phase or out-of-phase temperature synchronization helps reduce the energy consumed to keep room conditions at a comfortable level. At the same time, we consider the effect of the location of the sensor for temperature feedback control on synchronization, temperature distribution, and energy usage.

Phase synchronization of self-sustained oscillations in constituent subsystems is a phenomenon that may present itself in complex dynamical systems of different types. Huygens [7], in the 17th century, reported that the pendulums of two clocks could, under certain circumstances, swing "in sympathy." Since then, the phenomenon has been observed in other systems, especially in complex systems that are composed of interconnected subsystems [8–11]. It has been identified in various branches of the natural and social sciences, as well as engineering. In the natural sciences, examples such as the synchronization of the flashing of fireflies, the climatic history in Greenland and Antarctica [12], and physiological processes in humans [13–15] can be mentioned. In the social sciences, an example is the synchronization of an audience clapping at the end of a concert [16]. Three stages are observed: first, the audience applauds rapidly without synchronization; then, there is a decrease in frequency with synchronization; and finally, the frequency increases and breaks the synchronization. Other instances have been found in studies of the generation of opinions in a society, in the economic interaction between companies or countries, and in economic cycles [17].

There are examples of synchronization in mechanical [18–24], thermal [25], electrical and electronic [26] engineering, chemical systems [27], and generally in complex dynamical systems [8–10,28,29]. The synchronization of self-sustained oscillators in mechanical systems has been numerically studied for beams [30] and mathematical models using the van der Pol equation [31–34]. Aeronautical applications have been studied experimentally and numerically in fluidic oscillators [35], and the synchronization theory has been used to study thermoacoustic instability in a swirl-stabilized combustor [36]. Another example is the oscillatory behavior of local vortices, next to heat sources, that affects the thermal energy transfer to a downward transient flow in a vertical channel opposing mixed convection; this type of flow has been numerically studied [37] and is one of three possible solutions that depend on the Reynolds, Richardson, and Prandtl numbers, as well as the geometry of the channel. In short, in the last decades, the study of synchronization has generated a large quantity of theoretical and experimental information that has been reported in the literature.

There has been little experimental work, however, on the synchronization of self-sustained oscillations derived from sources of heat. One exception is the study of candle flames, which are known to flicker and oscillate in a self-sustaining manner, with the cause being attributed to instability in the buoyant flow near the base of the flame [38]. The flickering of arrays of candles can then synchronize in different ways, depending on geometrical parameters and initial conditions [39]. For example, three candles in a triangular array can exhibit four different dynamically synchronized oscillatory modes [40]: in-phase, partial in-phase, rotation, and death. In this and other cases, instability

Received 25 October 2018; revision received 2 October 2019; accepted for publication 3 February 2020; published online 9 March 2020.

*Graduate Student, Departamento de Termofluidos, Facultad de Ingeniería; mariosanlop@gmail.com.
†Professor, Departamento de Termofluidos, Facultad de Ingeniería; rchavezm@ingenieria.unam.mx.
‡Professor, Departamento de Termofluidos, Facultad de Ingeniería; jfso@unam.mx.
§Professor Emeritus, Department of Aerospace and Mechanical Engineering; Mihir.Sen.1@nd.edu.

is what induces flow and temperature oscillations through a Hopf bifurcation. Another way oscillations can occur in thermal systems is by active control of the temperature. This is indeed very common in industrial and domestic applications where temperature oscillations are often found. A thermal-hydraulic network was experimentally studied in Ref. [41]; and frequency locking, phase synchronization, and phase slips were observed in the flows in three secondary loops that were controlled by thermostats.

Thermostatic control of room temperature is commonly used for climate control in buildings. Typically, this is hysteretic; i.e., there is a deadband of temperature with the lower and upper limits controlling the on and off, respectively, of a heater (we will refer throughout to heating, although cooling is much the same). This leads to self-sustained temperature oscillations, and so it is important to look at the possibility of synchronization between the oscillations in adjacent rooms. In the past, this has been theoretically studied using lumped approximations for the cavities and a simplified conduction heat transfer between them [42–44]. Various dynamic modes have been predicted: a time invariant solution, and several in-phase and out-of-phase limits cycles. Strictly speaking, however, a complete analysis should also include three-dimensional natural convection; the onset of turbulence in the cavities; and transient heat conduction in the wall between them, which is a somewhat more difficult problem. In reality, subsystems are also not truly identical so that some lock-in in between subsystems must occur for synchronization to happen. For this reason, it is important to conduct laboratory experiments under controlled conditions, and that is the purpose of the present work.

Pikovsky et al. [29] defined synchronization as an "adjustment of rhythms of oscillating objects due to their weak interaction." Two oscillations are in phase synchronization if they have the same frequency and a constant phase difference between them. The phase difference may be zero (in which case, they are in phase), 180 deg (antiphase), or any other constant value. By definition, oscillations at different frequencies cannot enter into synchronization of this type.

This is a first attempt to study experimentally the thermal synchronization in cavities under controlled conditions. Here, we are interested in the phase synchronization of temperature oscillations and its effect on energy consumption and thermal comfort. For this to happen, there must be at least two similar subsystems with self-sustained oscillations that convert constant energy inputs into temperature oscillations, and there must be thermal interaction between the subsystems. In the problem studied here, there are two similar thermostatically controlled cavities that share a common wall, which is identical except for inevitable differences in construction. The cavities along with their respective control systems are the subsystems. Temperature oscillations are due to independent thermostatic control in each cavity. Thermal interaction is by conduction through the common wall for which the properties play an important role in the problem: if conduction is too weak, the temperature oscillations in the two cavities will be independent; and if it is too strong, the temperatures in the cavities will behave as one. Thermal diffusivity also plays a role in the time response of the wall as compared to that of convection in the cavities.

II. Experimental Aspects

The test facility involves the design and fabrication of two cavities with individual heaters, instrumentation for temperature measurement in each cavity, and independent thermostatic temperature control for each cavity. The technical specifications of the equipment are presented in Table 1. To minimize external influences from the laboratory where the experiment is carried out, the cavities are placed in an environmental chamber.

A. Design and Fabrication

Figures 1–4 show schematics of the setup that was fabricated and used for the experiments. Some of the details are described in the following:

The cavities are shown in Fig. 1. Each cavity is 56.30 mm (length) × 50 mm (width) × 50 mm (height) of inner dimensions with a tolerance of 0.05 mm. Numbers 1 and 2 denote the variables in the left and right cavities, respectively. All pieces were assembled using silicone sealant to provide an airtight seal. Each cavity has six walls, and these are of three types:

1) The first type is the common wall: This separates the two cavities and can be of different materials and thicknesses. The one used in the experiments is a square copper plate of 50 mm per side and 0.24 mm (thickness), as well as thermal resistance of $\approx 6.37 \times 10^{-7}$ $(\mathrm{m}^2 \cdot \mathrm{K})/\mathrm{W}$.

2) The second type is the heater wall: These are the outside walls made of 6-mm-thick acrylic that incorporate the electrical heaters. The electrical heaters are composed of nichrome ribbons coiled around 45×20 mm mica plates of 0.30 mm thickness. Each heater has a total electrical resistance of 1 Ω, and it is protected on both sides by other 50×25 mm mica plates. The total thickness of the heater is 3 mm. To ensure that most of the heat produced by the heaters is transferred to the interior of the cavities, the external faces of the acrylic were insulated with Styrofoam™ of 10 mm thickness.

3) The third type is the acrylic wall: There are four walls of this type in each cavity that are plates of 6 mm of thickness. Heat is transferred to the outside through these walls.

1. *Thermostat*

Each heater is independently controlled by a computer-operated thermostat; the control system is schematically shown in Fig. 2. The hardware of the thermostat is composed of a control stage and a power stage. The former is a data acquisition system that reads a temperature signal from the cavity, generates a digital signal to switch the heater on or off, and monitors the energy supplied to each cavity. The latter is a relay and a precision power source that does the actual heating, it communicates with the data acquisition system via a Universal Serial Bus (USB) wire; the heat rate generated is 2.70 W per heater. The control software and user interface of the thermostat were developed in LabVIEW™. The reading of the thermocouple is compared against the lower and upper temperature limits (T_L and T_U respectively) and a generated control signal, which is sent to a relay to open or close the power-stage electric circuit. The heater goes on when the temperature falls below T_L, and it goes off when it rises above T_U. This makes the temperature oscillate between the two limits that define the deadband: $\Delta T_{\mathrm{db}} = T_U - T_L$. The software also allows a choice of the instant that each heater is activated for the first time; so, for example, they can both be activated at the same instant of time, or the start of one of them can be delayed with respect to the other.

2. Computer

The computer with the data acquisition system are shown in Fig. 2. It runs the LabVIEW control program and saves data from the experiments. The following data were acquired and recorded at 1 sample/s: time t, chamber temperature T_c, maximum and minimum values of the temperatures for each cavity, control output for

Table 1 Technical specifications of the equipment

Device	Model	Description
Precision power source	Tektronix: PW4305	30 V ± 0.03%, 5 A ± 0.05%
Thermocouple amplifier module	National Instruments (NI) PXIe-4353 and TB 4353	— —
Digital I/O generator module	NI PXI-6528	— —
Relay	OMEGA OME-DB-24PR	Electromechanical relay 5 A, 30 V dc
Thermocouple wire	OMEGA, TT-T-30-SLE	Gauge 30 with special limit error, greater than 0.5°C or 0.4%
Thermistor sensor	ON-401-PP	0 to 70°C ± 0.1°C
Thermal bath	Witeg WCP-P8	−25 to 150°C ± 0.1°C

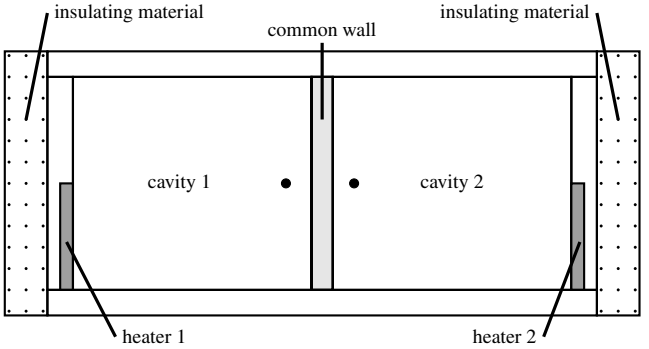

Fig. 1 Experimental model: cavities. A filled dot denotes a thermocouple.

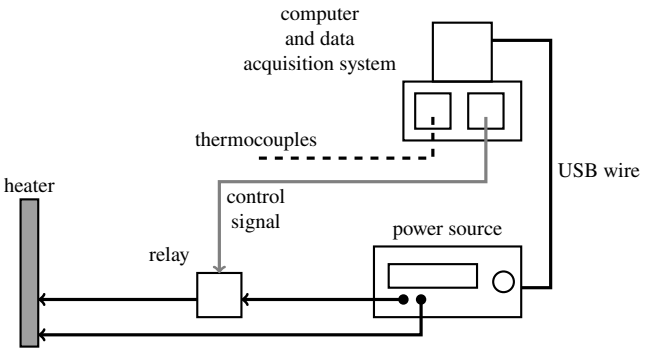

Fig. 2 Experimental setup: control system.

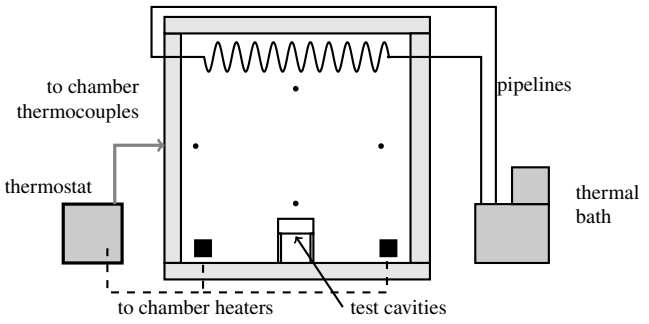

Fig. 3 Environmental chamber. Filled dots denote thermocouples.

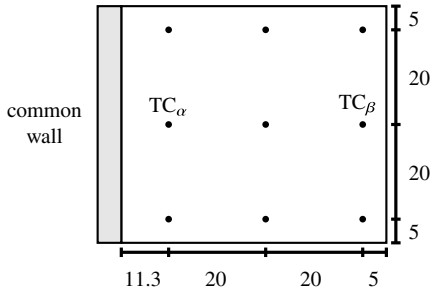

Fig. 4 Position of the thermocouples in cavity 2; thermocouples TC_α and TC_β are used for control in Sec. V.D. Distances are in millimeters.

each cavity (i.e., on or off), the nine thermocouple outputs for each cavity, and the voltage and current supplied by the power sources.

3. Environmental Chamber

To minimize the effect of temperature variation and air movements in the laboratory, the experimental model in Fig. 1 is placed in an environmental chamber shown in Fig. 3. This is a box of internal dimensions of $780 \times 780 \times 780$ mm in which the temperature T_c can be controlled between 20 and 25°C with a variation of ±0.10°C. The walls of this chamber are composite, the exterior wall is made of 6 mm acrylic, and the interior wall is made of 50 mm Styrofoam. The temperature of the chamber is controlled using a thermal bath and four chamber heaters. There is a heat exchanger coil at the roof of the chamber through which water circulates from the thermal bath at a temperature 1°C below the desired chamber temperature. T_c is corrected by the chamber heaters, which are located at the four corners of the chamber; each consists of an electrical resistance and a low flow fan to avoid setting up significant air currents within the chamber, and it provides a variable heating rate ranging from 0.50 to 10 W, according to need. Four type-T thermocouples were installed at different points of the median vertical plane and at a distance of 390 mm from the back wall. The average temperature of these thermocouples is compared with the set temperature to put the chamber heaters on or off.

4. Measurements

There are nine T-type thermocouples in each cavity located on a vertical plane, which is parallel to the rear wall of the cavity and located 25 mm from it. Figure 4 shows the thermocouples installed in cavity 2, which is located in a 3×3 matrix. The wire has a cross-sectional area of 0.47 mm^2, and its heat capacity is very small. The average time constant of the thermocouples is 5.30 s, which is measured in still air from 0 to 23.50°C; it is much smaller than the period of temperature oscillations. This ensures that the thermocouples can respond to the dynamic changes of temperature. According to the technical specifications of the data acquisition system and the type-T thermocouple, the accuracy of the temperature measurement system is 0.38°C. To improve the accuracy, they were calibrated in LabVIEW in the 10–50°C range in increments of 10°C. The readings were compared against a precision thermistor sensor to an accuracy of 0.10°C. After calibration, the readings of the thermocouples showed a standard deviation of 0.01°C at ambient temperature.

B. Operation

Some details of the experimental procedure are as follows:

1. Controls

There are different possibilities for the temperature control (TC) signal that can be used for control purposes: it can be either the temperature measured at a single location (TC_α or TC_β) or an average of several locations. Except for Sec. V.D, the results reported in this work were obtained using the readings of thermocouples TC_α as control inputs to the respective thermostat, which are shown in Fig. 4.

2. Runs

Each experiment starts by setting T_c and by waiting until the temperature inside the cavities is uniform and close to T_c. Then, T_L and T_U are set in the software. Unless otherwise specified, the experiments were carried out by activating the heaters at the same time. Each experiment is run long enough to make sure that the temperature oscillations reach steady conditions: from 24 to 50 h. Data are acquired during all of this interval; the temperatures of the left and right cavities are named $T_1(t)$ and $T_2(t)$, respectively. After completion of the run, the thermostat is turned off, and the apparatus cooled to stable conditions before the next run.

The temperature in the chamber T_c is set at 23°C. This temperature was chosen from the results of Sec. V.B, where the effect of T_c is studied. The upper and lower limits of the deadband are set in all the experiments to be 25 and 30°C, respectively; $\Delta T_{\text{db}} = 5$°C avoids flickering of the equipment and possible damage to the precision power sources. Previous tests have shown that $\Delta T_{\text{db}} = 5$°C or greater minimizes the overshoot of the temperature signal of the cavities.

III. Signal Analysis

The instantaneous frequency of a periodic signal f can be calculated from the reciprocal of the measured period τ of each oscillation; alternatively, a power spectral density can also be computed using many oscillations. The two methods give the same result. An important quantity is the phase difference between the two temperatures, which is measured as

$$\Delta\phi = 2\pi \frac{t_2 - t_1}{\tau} \tag{1}$$

where t_1 and t_2 are the instants of time when the temperatures of cavities 1 and 2 reach T_U, although any rising or falling fixed value between T_L and T_U can be used as reference. A positive (negative) $\Delta\phi$ indicates that the oscillations in cavity 1 lead (lag) cavity 2.

Synchronization between dynamic signals is commonly analyzed using the Kuramoto order parameter r [23,45]. First, the Hilbert transform $\hat{x}_i(t)$ is taken of the real signal $x_i(t)$ to give the complex analytic signal of $x_{ia}(t) = x_i(t) + i\hat{x}_i(t)$, where $i = \sqrt{-1}$. The instantaneous phase is then defined as

$$\phi_i(t) = \arctan \frac{\hat{x}_i(t)}{x_i(t)} \tag{2}$$

The instantaneous phase difference between signals $x_1(t)$ and $x_2(t)$ is calculated to be

$$\Delta\phi(t) = \phi_2(t) - \phi_1(t) \tag{3}$$

For periodic signals, Eqs. (1) and (3) give the same result, whereas Eq. (1) will not work for aperiodic signals.

The Kuramoto order parameter for the two signals is defined as

$$r(t) = \frac{1}{2}|(e^{i\phi_1(t)} + e^{i\phi_2(t)})| \tag{4}$$

The extremes of $r = 1$ and $r = 0$ indicate complete synchronization and a lack thereof, respectively.

Because the heater goes on and off periodically, the energy consumption was computed as the energy supplied every oscillation. This analysis includes the effect of $\Delta T = T_L - T_c$; the bigger the ΔT, the longer the time the heater is activated. So, the energy consumption of every oscillation is defined as

$$\mathrm{EC}_i = \frac{P \times t_{\mathrm{tc}}}{\tau} \tag{5}$$

where P is the power supplied to the electrical heater, t_{tc} is the time the heater is on, and τ is the period of the oscillation. The subscript i refers to cavity 1 or 2.

IV. Theory

A proper understanding of thermal synchronization requires the study of time-dependent convection inside each cavity. From a numerical perspective, it is necessary to solve the transient partial differential equations that represent the conservation of mass, momentum, and energy with their respective boundary and initial conditions. Some simplification can be made by assuming the flow to be two-dimensional. However, there are formidable obstacles to this approach. Experiments can be carried out for long periods of time (say, about a couple of days) with measurements every 1 s. Numerically, on the other hand, both short and long timescales have to be computed and stored. This is a stiff problem and presents an enormous burden for numerical computations. Furthermore, it is likely that the convection cells in the cavities may transition from laminar to turbulent; at which stage, unreliable turbulence models have to be used.

A different approach was taken by Sen [44], who developed a set of ordinary differential equations based on a lumped energy balance. The model can then be solved for the mean temperature in each cavity. The results show that there may be either in-phase or out-of-phase synchronization of the temperature oscillations. However, the lumped approach does not include all the physics present in the problem, such as the geometry of the rooms and the temperature distribution therein. The prediction of the simplified lumped model needs to be compared to experiments, and that is one of the motivations of the present study.

V. Experimental Results

A. Synchronization

Figure 5 shows the data from an experimental run carried out with $T_L = 25°\mathrm{C}$, $T_U = 30°\mathrm{C}$, $T_c = 23°\mathrm{C}$, and initial conditions of $T_1(0) = T_2(0) = 23.15°\mathrm{C}$. It can be seen in Fig. 5a that the temperatures of the cavities are synchronized from the beginning of the experiment. Figure 5b shows the instantaneous frequency. It is almost constant for the first 30 h of the experiment: increasing slightly during the last 10 h.

It can be seen in Fig. 5c that the values of $\Delta\phi$ fluctuate around +4 deg, which indicates that $T_1(t)$ leads $T_2(t)$ slightly. The same calculation is carried out when both cavities reach T_L; $\Delta\phi$ fluctuates around 0 deg, indicating that $T_1(t)$ and $T_2(t)$ are almost perfectly synchronized. Figure 5d shows a $T_1(t)$–$T_2(t)$ diagram with the arrows indicating the progress of time; i.e., as time advances, the point $(T_1(t), T_2(t))$ moves clockwise around a "quadrilateral" geometry. The width of the quadrilateral represents the phase difference between $T_1(t)$ and $T_2(t)$ because, for $\Delta\phi = 0$, the graph would be a straight line at 45 deg. Figure 5e shows that the value of the Kuramoto order parameter is $r = 1$ for the duration of the experiment.

The average energy consumption (EC) per oscillation can be observed in Fig. 5f. As can be seen this parameter is almost constant during the time the experiment is run; the ECs of cavities 1 and 2 are 0.91 and 0.94 W · h/oscillation, respectively, having a difference of 3.29% in the energy consumed by the cavities. In this case, cavity 1 leads cavity 2, meaning that the second needs more time to reach T_U, having as a consequence the use of more energy.

B. Effect of Environmental Chamber Temperature

To study the effect of T_c on the synchronization of the cavities, the experiments were carried out with $T_L = 25°\mathrm{C}$ and $T_U = 30°\mathrm{C}$; T_c was set at temperatures from 21 to 24°C in increments of 1°C. The temperature control of both rooms was activated at the same time.

Figure 6 shows the variation of the oscillation frequency f for each T_c. As T_c is increased, f diminishes. This is because the cooling from the interior of the cavities to the environmental chamber is diminished with the decrease in the driving temperature difference; as a consequence, the heaters work less often. Cavities 1 and 2 have similar frequencies at 24°C; but, when T_c is decreased to 21°C, the frequency of cavity 2 is 0.23% lower due to the slight difference in construction between them. Figure 7 is a T_1–T_2 diagram. For 21°C, the temperature oscillations of the cavities have $\Delta\phi = 54$ deg. For $T_c = 22°\mathrm{C}$, the direction of motion is reversed and the geometry of the T_1–T_2 diagram is modified. For 23 and 24°C, the out-of-phase angle diminishes, oscillating around zero. The T_1–T_2 diagram is the thick line at 45 deg to the x axis, when the temperatures of both cavities reach T_U. We have chosen $T_c = 23°\mathrm{C}$ because the phase difference between the temperature oscillations of the two cavities is then almost zero, and we can clearly observe the effect of variation of the other parameters.

For all cases, the EC is almost constant; Table 2 shows the average energy consumption per oscillation for all T_c. As can be seen, the higher the temperature in the environmental chamber, the less energy is necessary to keep the temperature in the specified range. As ΔT diminishes, the energy consumed by the cavities tends to be the same.

C. Effect of Instants of Activation

In this section, the effect on the synchronization of instants of activation of the heaters is analyzed with $\Delta T = 5°\mathrm{C}$ and $T_c = 23°\mathrm{C}$. These were varied in the following manner:

1) For case A, the temperature control of both cavities is activated at the same instant with $T_1(0) = T_2(0) = 23.15°\mathrm{C}$.

2) For case B_1, both heaters are activated at the same instant with $T_1(0) = 25°\mathrm{C}$ and $T_2(0) = 30°\mathrm{C}$.

3) For case B_2, both heaters are activated at the same instant with $T_1(0) = 30°\mathrm{C}$ and $T_2(0) = 25°\mathrm{C}$.

4) For case C_1, heater 1 activated at $t = 0$ with $T_1(0) = T_2(0) = 23.08°\mathrm{C}$, and cavity 2 activated when $T_1 = 30°\mathrm{C}$.

5) For case C_2, heater 2 activated at $t = 0$ with $T_1(0) = T_2(0) = 23.17°\mathrm{C}$, and cavity 1 activated when $T_2 = 30°\mathrm{C}$.

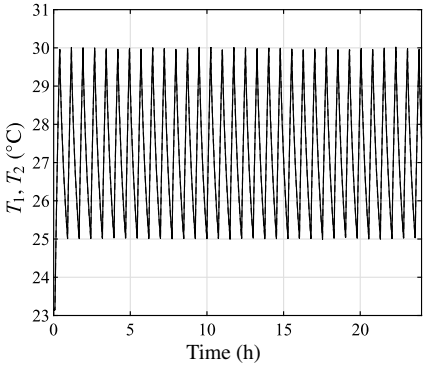

a) Temperatures $T_1(t)$ and $T_2(t)$

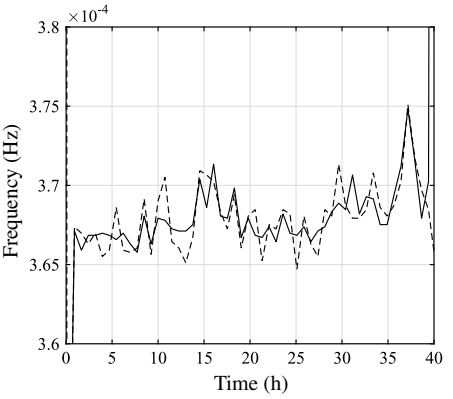

b) Frequency spectra of $T_1(t)$ and $T_2(t)$

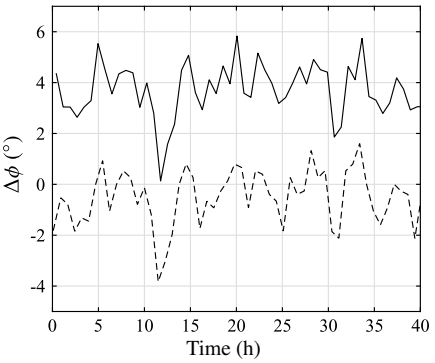

c) Phase difference $\Delta\phi(t)$, T_U (solid line) and T_L (dashed line)

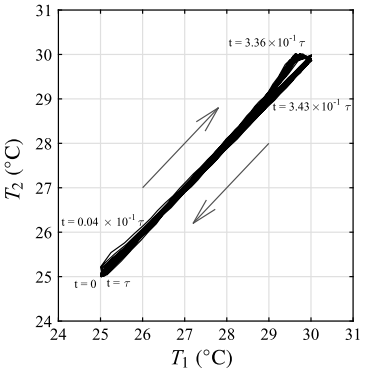

d) T_1 vs T_2

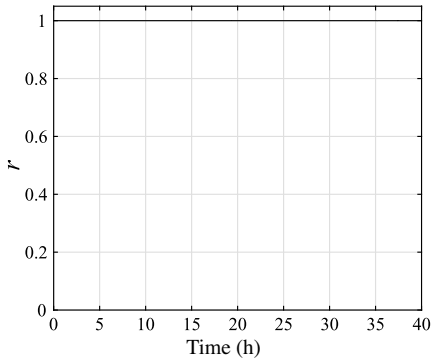

e) Kuramoto order parameter r

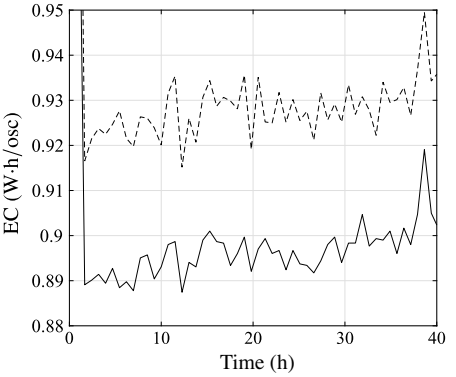

f) Energy consumption per oscillation

Fig. 5 Experimental results for $T_c = 23$°C: cavity 1 (solid lines), and cavity 2 (dashed lines).

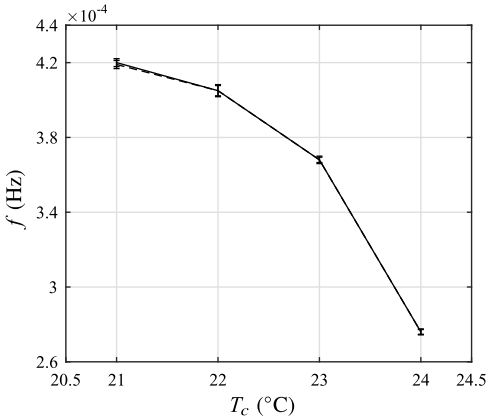

Fig. 6 Oscillation frequency f: cavity 1 (solid lines), and cavity 2 (dashed lines).

The results for case A are shown in Fig. 5b, in which it can be seen that the frequencies of the oscillations in both cavities are similar and lie between 3.65×10^{-4} and 3.70×10^{-4} Hz during the first 30 h after start. Figures 8a–8d show the results for case B_2. Figure 8a shows the first 15 h experiment; the first 13 h are necessary for the oscillations to stabilize. After this time, $T_1(t)$ is seen to lead $T_2(t)$, as seen in Fig. 8b. The frequency of oscillation of each cavity increases slowly until it reaches 3.65×10^{-4} Hz, which is close to that in case A, as shown in Fig. 8c. With respect to the phase angle, Fig. 8d shows that $T_2(t)$ initially lags $T_1(t)$; then, the condition is reversed, reaching $\Delta\phi = -175$ deg. With the passage of the time, $\Delta\phi$ increases until finally it oscillates around zero. In Fig. 8e, it can be observed that the energy used per oscillation increases as $\Delta\phi$ tends to zero; i.e., at the beginning of the experiment, the thermal interaction between cavities helps to decrease the energy consumption.

Table 3 shows a summary of the results for different initial conditions. It can be seen that the frequency of oscillation is independent of the initial activation condition of the heaters (i.e., on or off).

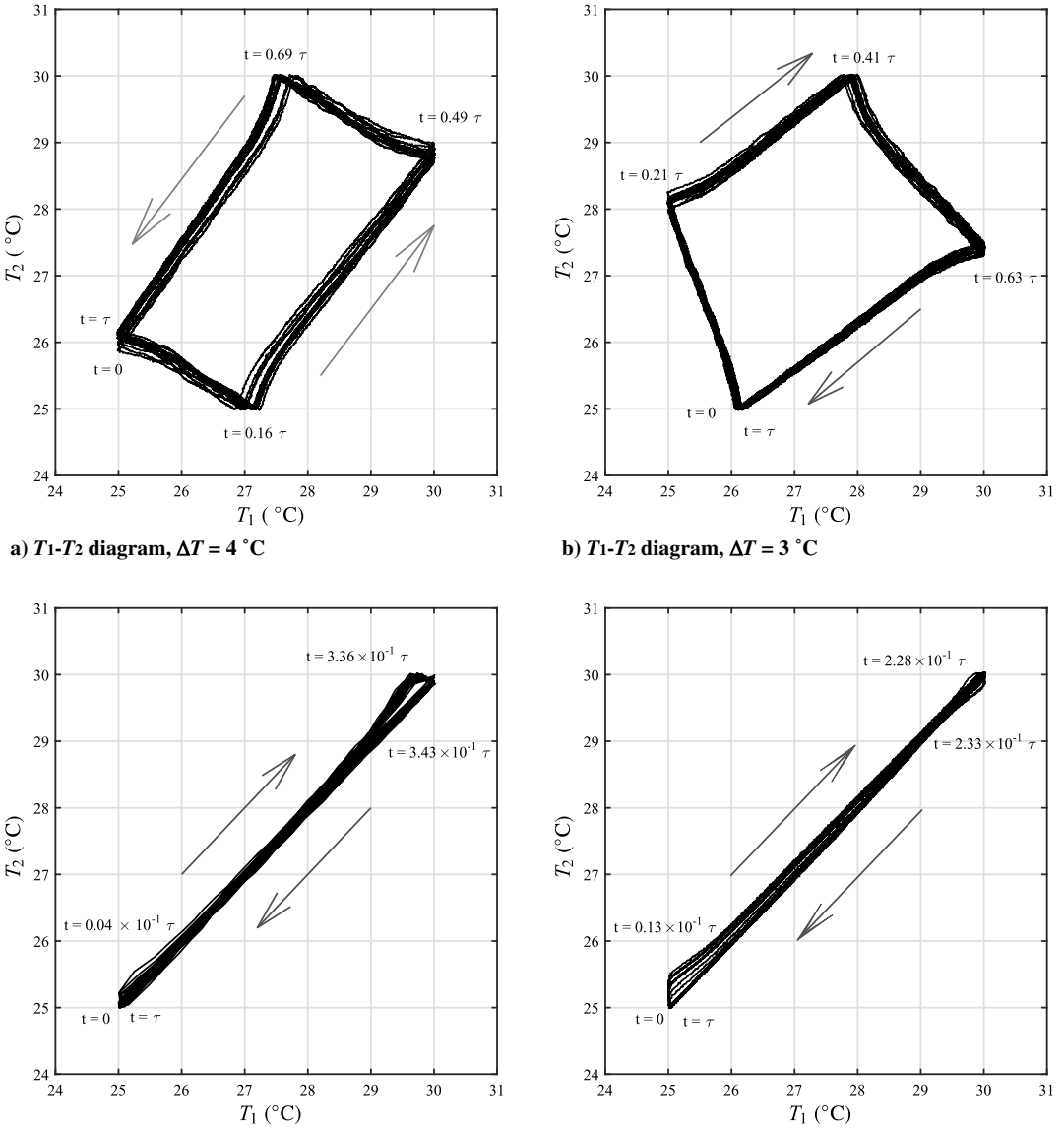

a) T_1-T_2 diagram, ΔT = 4 °C

b) T_1-T_2 diagram, ΔT = 3 °C

c) T_1-T_2 diagram, ΔT = 2 °C

d) T_1-T_2 diagram, ΔT = 1 °C

Fig. 7 Effect of outside temperature; T_c = a) 21°C, b) 22°C, c) 23°C, and d) 24°C.

It should be pointed out that, for all initial conditions, after the stabilization time studied, the temperature of cavity 1 leads that of cavity 2: except for case A, for which $\Delta\phi = -0.39$ deg.

The time necessary to reach steady conditions for all the instants of activation studied is shown in Fig. 9. For cases B_1 and C_2, $\Delta\phi$ does not present a transition from positive to negative, resulting in a quicker stabilization. For the other cases, approximately 20 h are necessary to reach steady conditions.

D. Effect of Choice of Temperature Control Signal

In this section, the effect of the choice of the temperature input of the thermostat on the synchronization is studied. As mentioned in previous sections, nine thermocouples were installed in each cavity; and any of these can be used as input of the thermostat.

Table 2 Energy consumption of cavities

T_c, °C	EC_1, W · h/osc	EC_2, W · h/osc	Δ EC, %
20	1.56	1.69	8.33
21	1.35	1.41	4.44
22	1.11	1.09	1.80
23	0.91	0.94	3.29
24	0.60	0.62	3.33

Experiments were performed for the following cases: all with $T_L = 25$°C, $T_U = 30$°C, and $T_c = 24$°C.

1) For case D, the control signal is from thermocouple TC_α; $T_1(0) = T_2(0) = 24.15$°C.

2) For case E, the control signal is from thermocouple TC_β; $T_1(0) = T_2(0) = 23.83$°C.

3) For case F, the control signal is the average temperature of the nine thermocouples; $T_1(0) = T_2(0) = 23.85$°C.

The results for case D show that the instantaneous frequency has a similar behavior for each cavity with an average of $f = 2.75 \times 10^{-4}$ Hz. The T_1–T_2 diagram for these conditions is shown in Fig. 7d. Synchronization of the temperatures is confirmed by the Kuramoto order parameter that has a value of one, as shown in Fig. 10a.

For case E, the temperatures have a phase difference between them that is more evident as time goes on, affecting the Kuramoto order parameter r for which the value is close to one, as shown in Fig. 10b. The minimum value of r corresponds to the maximum phase difference of temperature. The ratio $f_1/f_2 = 1.04$, which means that, after 26 oscillations of cavity 1 and 25 of cavity 2, the temperatures coincide again.

For case F, the frequencies of oscillation are $f_1 = 3.35 \times 10^{-4}$ Hz and $f_2 = 3.28 \times 10^{-4}$ Hz with the ratio $f_1/f_2 = 1.02$. Now, 51 oscillations of cavity 1 and 50 for cavity 2 (approximately 42 h) are needed for the temperatures to overlap again. This is nearly twice

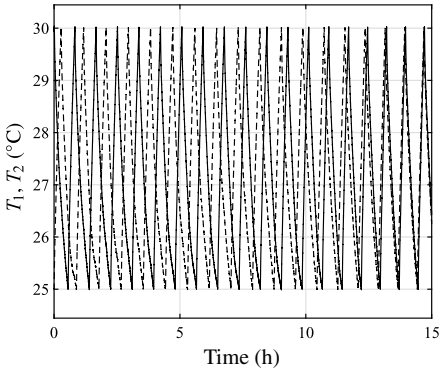

a) Temperature initial time

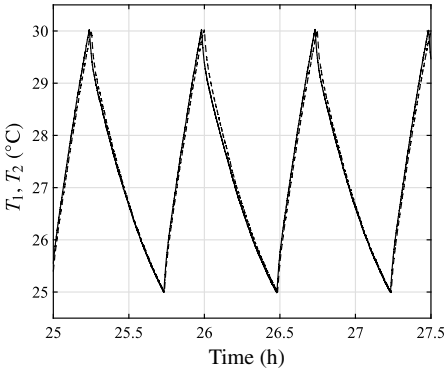

b) Temperature after 20 h

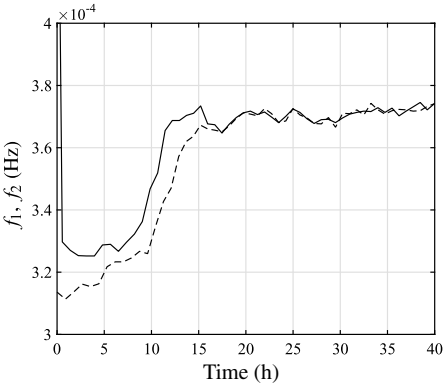

c) Frequency of temperature oscillation

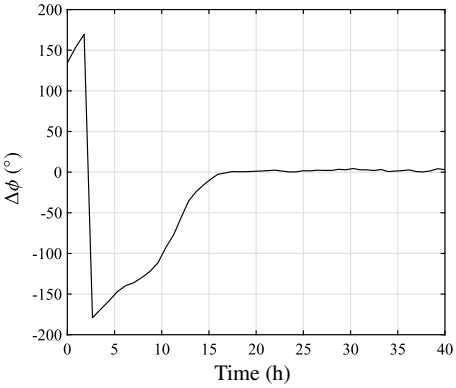

d) Out-of-phase angle

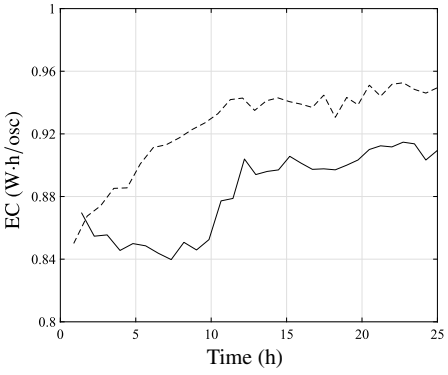

e) Evolution of energy consumption per oscillation

Fig. 8 Experimental results case B_2: cavity 1 (solid lines), and cavity 2 (dashed lines).

the time than in case E. The Kuramoto order parameter r is also affected, as depicted in Fig. 10c. Table 4 is a summary of the frequencies of oscillation of the three control signals and their ratios.

As mentioned before for case E, there is an increase in phase difference between the temperature oscillations, leading to greater thermal interaction between them so that the time necessary to reach T_L or T_U is larger; i.e., the frequency of oscillation decreases. On the other hand, as the phase difference decreases, the frequency of oscillation increases. This has the effect of changing the frequency of oscillation considerably, as in Fig. 11. Another important effect is the energy consumption; case E is the one that consumes less energy. On the other hand, case D is the case that consumes more energy because the temperature in cavities is synchronized and the thermal interaction between them is minimum; the energy consumed per

Table 3 Effect of instants of activation

Cases	$f_1 \times 10^4$, Hz	$f_2 \times 10^4$, Hz	$\Delta\phi$, deg	t_s, h
A	3.68	3.68	−0.39	0
B_1	3.91	3.64	3.09	7.80
B_2	3.70	3.70	1.47	17.50
C_1	3.71	3.69	3.07	18
C_2	3.65	3.66	3.87	12.30

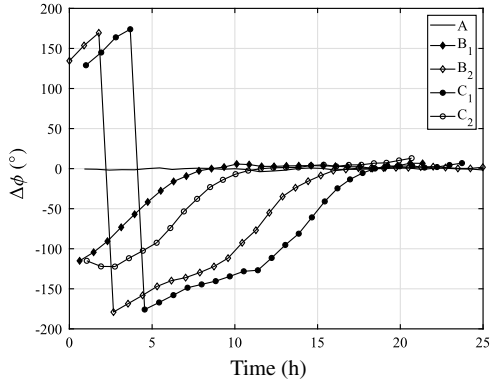

Fig. 9 Evolution of out-of-phase angle.

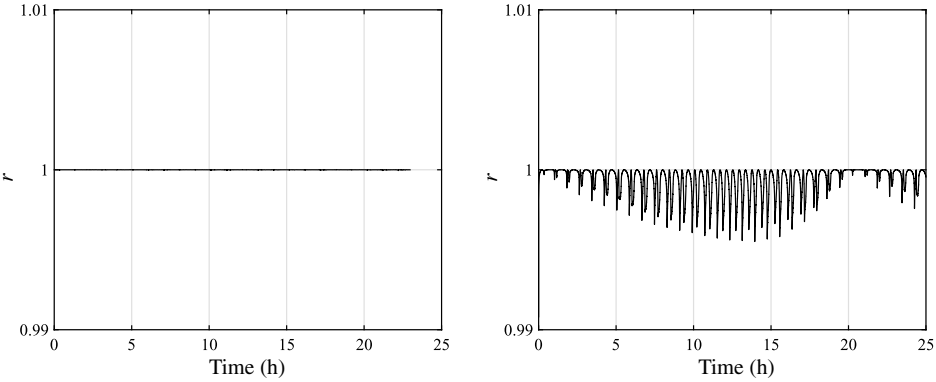

a) Thermocouple TC$_\alpha$ **b) Thermocouple TC$_\beta$**

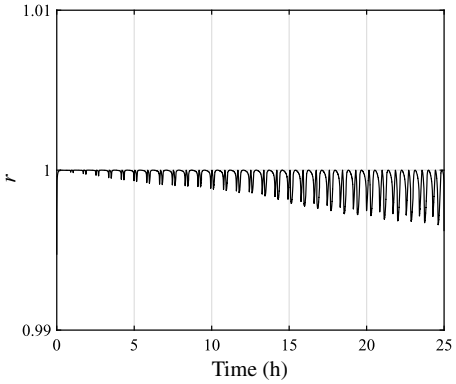

c) Average temperature

Fig. 10 Kuramoto order parameter r: effect of control temperature location.

Table 4 Effect of choice of temperature control signal

Cases	$f_1 \times 10^4$, Hz	$f_2 \times 10^4$, Hz	f_1/f_2	EC$_1$, W · h/osc	EC$_2$, W · h/osc
D	2.75	2.75	1.00	0.60	0.62
E	3.47	3.32	1.04	0.44	0.49
F	3.35	3.28	1.02	0.54	0.55

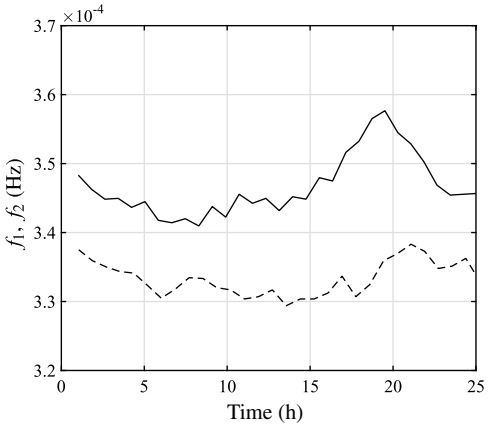

Fig. 11 Instantaneous frequency for control signal case E, in Sec. V.D: cavity 1 (solid lines), and cavity 2 (dashed lines).

oscillation is 36.36% larger for cavity 1 and 26.53% larger for cavity 2. The results of the energy consumption are shown in Table 4.

Looking at the temperature in cavity 1, when T_U is reached, it is seen that, for case D, the average temperature is 31.47°C; whereas for cases E and F, is the average temperatures are 29.01 and 30°C, respectively. In general, the temperature at all measurement points within the cavity is larger for case D; this makes necessary the use of more energy, as pointed out in previous paragraphs. The thermocouples used to control the thermostat and the heaters are located at opposite extremes of the cavity so that the heat transferred by convection takes time to reach thermocouple TC$_\alpha$. This implies that it takes longer to reach T_L, and thus its frequency of oscillation is smaller than those for cases E and F. On the other hand, a lower-temperature distribution is found in case F and is the one with the largest ratio f_1/f_2. So, it can be deduced that a higher-temperature distribution in the cavity, mainly next to the common wall, promotes the synchronization of the cavities.

VI. Conclusions

It has been known that self-sustained oscillations in a system with coupled subsystems can lead to synchronization among the oscillations. Previous theoretical work has shown that there are reasons to believe that there would also be synchronization of temperature oscillations in thermally connected cavities, but this has not been experimentally observed up to now. The lumped analysis in Refs. [42–44] indicates some of the physics behind the temperature oscillations. However, aspects such as cellular convection (and consequent delay between the temperature reading by the thermocouple and actuation of the heater) are not taken into account.

The lumped analysis uses three nondimensional parameters that govern the system related to the heat transfer coefficient, as well as the upper and lower temperature limits. In addition, however, there are parameters that are not present in a lumped analysis: the fluid Prandtl number and cavity Rayleigh number. It is possible to change some of the groups during experimentation but not all. For example, for a full-scale building, the Prandtl number will be the same but the Rayleigh number will be different.

The objective of this experimental study was to find if the synchronization of temperature exists. Two cavities were constructed for this purpose, which were made similar as far as possible. Temperature oscillations were induced by a hysteretic thermostat in each cavity. The temperature oscillations turned out to be synchronized with $\Delta\phi \approx +4$ deg. The laboratory experiments reported here confirmed the existence of this synchronization for certain geometries, material

properties, and initial conditions. Two cavities with a common wall were chosen for experimentation; the temperature in each oscillated due to hysteretic thermostatic control. Synchronization was observed both with and without a phase difference between the two oscillations. The effect of the wall conduction and the choice of control temperature have been noted. The characteristics of the actual synchronization are slightly different from those of the theoretical lumped parameter analysis.

The presence or absence of synchronization will have an effect on the strength of the supply of heating (or cooling) in buildings. The results are of interest in climate control, especially from the point of view of energy usage. The instantaneous energy consumption during heating is the sum of the energy supplied to each cavity. For this reason, the out-of-phase temperature oscillations require less installed capacity of the heater as compared to the in-phase temperature oscillations. The information obtained from scale models, such as that here, will be useful in the design of heating in full-scale buildings.

Acknowledgments

The authors acknowledge financial aid from the Support Program for Research and Technological Innovation Projects of the National Autonomous University of Mexico (UNAM) under contract number IN114216. The experiments were carried out in Thermofluid Research Laboratory, Faculty of Engineering, at the UNAM.

References

[1] Cao, X., Dai, X., and Liu, J., "Building Energy-Consumption Status Worldwide and the State-of-the-Art Technologies for Zero-Energy Buildings During the Past Decade," *Energy and Buildings*, Vol. 128, Sept. 2016, pp. 198–213. https://doi.org/10.1016/j.enbuild.2016.06.089

[2] Lu, M., and Lai, J. H., "Building Energy: A Review on Consumptions, Policies, Rating Schemes and Standards," *Energy Procedia, Innovative Solutions for Energy Transitions*, Vol. 158, Feb. 2019, pp. 3633–3638. https://doi.org/10.1016/j.egypro.2019.01.899

[3] Sarbu, I., and Adam, M., "Experimental and Numerical Investigations of the Energy Efficiency of Conventional Air Conditioning Systems in Cooling Mode and Comfort Assurance in Office Buildings," *Energy and Buildings*, Vol. 85, Dec. 2014, pp. 45–58. https://doi.org/10.1016/j.enbuild.2014.09.022

[4] Fantucci, S., Lorenzati, A., Capozzoli, A., and Perino, M., "Analysis of the Temperature Dependence of the Thermal Conductivity in Vacuum Insulation Panels," *Energy and Buildings*, Vol. 183, Jan. 2019, pp. 64–74. https://doi.org/10.1016/j.enbuild.2018.10.002

[5] Liu, F., Zhu, J., Liu, J., Ma, B., Zhou, W., and Li, R., "Preparation and Properties of Capric-Stearic Acid/White Carbon Black Composite for Thermal Storage in Building Envelope," *Energy and Buildings*, Vol. 158, Jan. 2018, pp. 1781–1789. https://doi.org/10.1016/j.enbuild.2017.09.076

[6] Zeng, Q., Mao, T., Li, H., and Peng, Y., "Thermally Insulating Lightweight Cement-Based Composites Incorporating Glass Beads and Nano-Silica Aerogels for Sustainably Energy-Saving Buildings," *Energy and Buildings*, Vol. 174, Sept. 2018, pp. 97–110. https://doi.org/10.1016/j.enbuild.2018.06.031

[7] Huygens, C., *Letter to de Sluse. Letter No. 1333 of February 24, 1665, page 241*, Vol. 5, Soc. Hollandaise des Sciences, Martinus–Nijhoff, The Hague, The Netherlands, 1673, pp. 1664–1665.

[8] Mosekilde, E., Mainstrenko, Y., and Postnov, D., *Chaotic Synchronization: Applications to Living Systems*, World Scientific, Singapore, ROS, 2002. https://doi.org/10.1142/4845

[9] Strogatz, S., *Sync: The Emerging Science of Spontaneous Order*, Hyperion Press, New York, 2004. https://doi.org/10.1063/1.1784276

[10] Manrubia, S., Mikhailov, A., and Zenette, D., *Synchronization: A Universal Complex in Nonlinear Sciences*, World Scientific, Singapore, ROS, 2001.

[11] Balanov, A., Janson, N., Postnov, D., and Sosnovtseva, O., *Synchronization: From Simple to Complex*, Springer, Berlin, 2009. https://doi.org/10.1007/978-3-540-72128-4

[12] Oh, J., Reischmann, E., and Rial, J., "Polar Synchronization and the Synchronization Climatic History of Greenland and Antarctica," *Quaternary Science Reviews*, Vol. 83, Jan. 2014, pp. 129–142. https://doi.org/10.1016/j.quascirev.2013.10.025

[13] Glass, L., "Synchronization and Rhythmic Processes in Physiology," *Nature*, Vol. 410, Jan. 2001, pp. 277–284. https://doi.org/10.1038/35065745

[14] Buck, J., and Buck, E., "Synchronous Fireflies," *Scientific American*, Vol. 234, No. 5, 1976, pp. 74–85. https://doi.org/10.1038/scientificamerican0576-74

[15] Strogatz, S., and Stewart, I., "Coupled Oscillators and Biological Synchronization," *Scientific American*, Vol. 269, No. 6, 1993, pp. 102–109. https://doi.org/10.1038/scientificamerican1293-102

[16] Néda, Z., Ravasz, E., Brechet, Y., Vicsek, A., and Barabási, A., "Self-Organizing Processes: The Sound of Many Hands Clapping—Tumultuous Applause Can Transform Itself into Waves of Synchronized Clapping," *Nature*, Vol. 403, No. 6772, 2000, pp. 849–850. https://doi.org/10.1038/35002660

[17] Arenas, A., Díaz-Guilera, A., Kurths, J., Moreno, Y., and Zhou, C., "Synchronization in Complex Networks," *Physics Reports*, Vol. 469, No. 3, 2008, pp. 93–153. https://doi.org/10.1016/j.physrep.2008.09.002

[18] Bennett, M., Schatz, M., Rockwood, H., and Wiesenfeld, K., "Huygens's Clocks," *Proceedings of the Royal Society of London, Series A: Mathematical, Physical and Engineering Sciences*, Vol. 458, No. 2019, 2002, pp. 563–579. https://doi.org/10.1098/rspa.2001.0888

[19] Stefański, A., and Kapitaniak, T., "Synchronization of Mechanical Systems Driven by Chaotic or Random Excitation," *Journal of Sound and Vibration*, Vol. 260, No. 3, 2003, pp. 565–576. https://doi.org/10.1016/S0022-460X(02)01049-0

[20] Senator, M., "Synchronization of Two Coupled Escapement-Driven Pendulum Clocks," *Journal of Sound and Vibration*, Vol. 291, No. 3, 2006, pp. 566–603. https://doi.org/10.1016/j.jsv.2005.06.018

[21] Czolczynski, K., Perlikowski, P., Stefanski, A., and Kapitaniak, T., "Clustering of Huygens' Clocks," *Progress of Theoretical Physics*, Vol. 122, No. 4, 2009, pp. 1027–1033. https://doi.org/10.1143/PTP.122.1027

[22] Jáuregui, J., Sen, M., and López-Cajún, C., "Experimental Characterization of Synchronous Vibrations of Blades," *Proceedings of the ASME: Turbo Expo 2011*, Vol. 6, Pts. A–B, American Society of Mechanical Engineers, Fairfield, NJ, 2012, pp. 821–828. https://doi.org/10.1115/GT2011-46105

[23] González-Cruz, C., Jáuregui-Correa, J., López-Cajún, C., Domínguez-González, A., and Sen, M., "Experimental Analysis of Synchronization and Dynamics in an Automobile as a Complex System," *Mechanical Systems and Signal Processing*, Vol. 60, Aug. 2015, pp. 472–484. https://doi.org/10.1016/j.ymssp.2014.12.028

[24] Sen, M., and López-Cajún, C., "Review of Synchronization in Mechanical Systems," *Nonlinear Structural Dynamics and Damping*, edited by J. Jáuregui, Springer, New York, 2019, pp. 45–70.

[25] Barron, M., and Sen, M., "Synchronization of Temperature Oscillations in Heated Plates with Hysteretic On-Off Control," *Applied Thermal Engineering*, Vol. 65, No. 1, 2014, pp. 337–342. https://doi.org/10.1016/j.applthermaleng.2014.01.026

[26] Verrelli, C., "Synchronization of Permanent Magnetic Electric Motors: New Nonlinear Advances Results," *Nonlinear Analysis: Real World Applications*, Vol. 13, No. 1, 2012, pp. 395–409. https://doi.org/10.1016/j.nonrwa.2011.07.051

[27] Wang, J., and Chen, A., "Partial Synchronization in Coupled Chemical Chaotic Oscillator," *Journal of Computational and Applied Mathematics*, Vol. 233, No. 8, 2010, pp. 1897–1904. https://doi.org/10.1016/j.cam.2009.09.026

[28] Pecora, L., Carroll, T., Johnson, G., Mar, D., and Heagy, J., "Fundamentals of Synchronization in Chaotic Systems, Concepts and Applications," *Chaos*, Vol. 7, No. 4, 1997, pp. 520–543. https://doi.org/10.1063/1.166278

[29] Pikovsky, A., Rosenblum, M., and Kurths, J., *Synchronization: A Universal Concept in Nonlinear Sciences*, Cambridge Univ. Press, New York, 2001. https://doi.org/10.1017/CBO9780511755743

[30] Barron, M., and Sen, M., "Synchronization of Coupled Self-Excited Elastic Beams," *Journal of Sound and Vibration*, Vol. 324, No. 1, 2009, pp. 209–220. https://doi.org/10.1016/j.jsv.2009.02.007

[31] Barron, M., and Sen, M., "Synchronization of Four Coupled van der Pol Oscillators," *Nonlinear Dynamics*, Vol. 56, No. 4, 2008, pp. 357–367. https://doi.org/10.1007/s11071-008-9402-y

[32] Barron, M., and Sen, M., "Dynamic Behavior of a Large Ring of Coupled Self-Excited Oscillators," *Journal of Computational and Nonlinear Dynamics*, Vol. 8, No. 3, 2013, Paper 034501. https://doi.org/10.1115/1.4023008

[33] Vinod, V., Balaram, B., Narayanan, M., and Sen, M., "Effect of Oscillator and Initial Condition Differences in the Dynamics of a Ring of Dissipative Coupled van der Pol Oscillators," *Journal of Mechanical Science and Technology*, Vol. 29, No. 5, 2015, pp. 1931–1939. https://doi.org/10.1007/s12206-015-0103-4

[34] Vinod, V., Balaram, B., Narayanan, M., and Sen, M., "Effect of Configuration Symmetry on Synchronization in a Van der Pol Ring with Nonlocal Interactions," *Nonlinear Dynamics*, Vol. 89, No. 3, 2017, pp. 2103–2114. https://doi.org/10.1007/s11071-017-3572-4

[35] Tomac, M. N., and Gregory, J. W., "Phase-Synchronized Fluidic Oscillator Pair," *AIAA Journal*, Vol. 57, No. 2, 2019, pp. 670–681. https://doi.org/10.2514/1.J057065

[36] Pawar, S. A., Mondal, S., George, N. B., and Sujith, R. I., "Temporal and Spatiotemporal Analyses of Synchronization Transition in a Swirl-Stabilized Combustor," *AIAA Journal*, Vol. 57, No. 2, 2019, pp. 836–847. https://doi.org/10.2514/1.J057143

[37] Martnez-Suástegui, L., Treviño, C., and Cajas, J. C., "Thermal Nonlinear Oscillator in Mixed Convection," *Physical Review E*, Vol. 84, No. 4, 2011, Paper 046310. https://doi.org/10.1103/PhysRevE.84.046310

[38] Maxworthy, T., "The Flickering Candle: Transition to a Global Oscillation in a Thermal Plume," *Journal of Fluid Mechanics*, Vol. 390, July 1999, pp. 297–323. https://doi.org/10.1017/S002211209900508X

[39] Kitahata, H., Taguchi, J., Nagayama, M., Sakurai, T., Ikura, Y., Osa, A., Sumino, Y., Tanaka, M., Yokoyama, E., and Miike, H., "Oscillation and Synchronization in the Combustion of Candles," *Journal of Physical Chemistry A*, Vol. 113, No. 29, 2009, pp. 8164–8168. https://doi.org/10.1021/jp901487e

[40] Okamoto, K., Kijima, A., Umeno, Y., and Shima, H., "Synchronization in Flickering of Three-Coupled Candle Flames," *Scientific Reports*, Vol. 6, Oct. 2016, Paper 36145. https://doi.org/10.1038/srep36145

[41] Cai, W., Sen, M., Yang, K., and McClain, R., "Synchronization of Self-Sustained Thermostatic Oscillations in a Thermal-Hydraulic Network," *International Journal of Heat and Mass Transfer*, Vol. 49, No. 23, 2006, pp. 4444–4453. https://doi.org/10.1016/j.ijheatmasstransfer.2006.04.027

[42] Cai, W., and Sen, M., "Synchronization of Thermostatically Controlled First-order Systems," *International Journal of Heat and Mass Transfer*, Vol. 51, No. 11, 2008, pp. 3032–3043. https://doi.org/10.1016/j.ijheatmasstransfer.2007.09.010

[43] O'Brien, J., "Behavior, Prediction and Control of Thermostatically-Controlled, Thermally-Coupled Self-Excited Oscillators," B.S. Thesis, Dept. of Aerospace and Mechanical Engineering, Univ. of Notre Dame, Notre Dame, IN, 2012.

[44] Sen, M., "Effect of Walls on Synchronization of Thermostatic Room-Temperature Oscillations," *Journal of the Mexican Society of Mechanical Engineering*, Vol. 4, No. 3, 2012, pp. 81–88.

[45] González-Cruz, C., Jáuregui-Correa, J., Domínguez-González, A., and Lozano-Guzmán, A., "Effect of the Coupling Strength on the Nonlinear Synchronization of a Single-Stage Gear Transmission," *Nonlinear Dynamics*, Vol. 85, No. 1, 2016, pp. 123–140. https://doi.org/10.1007/s11071-016-2673-9